The influence of ruthenium on the magnetic properties of γ-Fe_2O_3 (maghemite) studied by Mössbauer spectroscopy

2003 J. Phys.: Condens. Matter 15 2907

(http://iopscience.iop.org/0953-8984/15/17/338)

INSTITUTE OF PHYSICS PUBLISHING JOURNAL OF PHYSICS: CONDENSED MATTER

J. Phys.: Condens. Matter **15** (2003) 2907–2915 PII: S0953-8984(03)56049-0

The influence of ruthenium on the magnetic properties of γ-Fe_2O_3 (maghemite) studied by Mössbauer spectroscopy

Örn Helgason[1], Jean-Marc Greneche[2], Frank J Berry[3] and Frederick Mosselmans[4]

[1] Science Institute, University of Iceland, Dunhagi 3, IS-107 Reykjavik, Iceland
[2] LPEC, UMR 6087, Université du Maine, 72085 Le Mans Cedex 9, France
[3] Department of Chemistry, The Open University, Walton Hall, Milton Keynes MK7 6AA, UK
[4] CLRC Daresbury Laboratory, Daresbury, Warrington WA4 4AD, UK

Received 14 November 2002
Published 22 April 2003
Online at stacks.iop.org/JPhysCM/15/2907

Abstract

Ruthenium-doped γ-Fe_2O_3 has been synthesized and examined by x-ray powder diffraction, XANES, EXAFS and by ^{57}Fe Mössbauer spectroscopy. Ruthenium K-edge x-ray absorption spectroscopy shows that ruthenium adopts a fully occupied octahedral site in the spinel related γ-Fe_2O_3 structure as Ru^{4+}. The ^{57}Fe Mössbauer spectra recorded in the presence of a longitudinal magnetic field of 6 T confirmed the octahedral coordination of the tetravalent ions and canting angles for the Fe^{3+} ions were determined as 24° for those in octahedral sites and 33° for those in tetrahedral sites. The ^{57}Fe Mössbauer spectra recorded *in situ* from ruthenium-doped γ-Fe_2O_3 showed parameters typical of maghemite up to 600 K but with a magnetic hyperfine field distribution suggesting an inhomogeneous distribution of ruthenium within particles of varied size around about 15 nm. At 700 K a phase transition from γ-Fe_2O_3 to α-Fe_2O_3 was observed and further studies showed the ruthenium-doped α-Fe_2O_3 to have a Morin transition temperature of about 400 K.

(Some figures in this article are in colour only in the electronic version)

1. Introduction

Mössbauer spectroscopy is a powerful tool to distinguish between magnetic iron oxides like Fe_3O_4, (magnetite), γ-Fe_2O_3, (maghemite) and α-Fe_2O_3, (hematite) and to study possible phase transitions and redox processes between these oxides [1, 2]. The iron(III) oxide γ-Fe_2O_3, maghemite, adopts a spinel-related structure commonly represented by the formula $(Fe)[Fe_{5/3}\Delta_{1/3}]O_4$, where ( ) denotes tetrahedral sites, [ ] indicates octahedral sites and Δ denotes vacancies. Besides its importance in processes concerning the exsolution and oxidation of titanomagnetite in geochemistry and paleomagnetism [1, 3–5], γ-Fe_2O_3 has

attracted attention because of its application in magnetic tape recording materials [6]. Doping of the material by metals such as trivalent aluminium [7, 8], magnesium and gadolinium [9], and also by cobalt and nickel to improve the magnetic performance [10], has been of interest for some years. Doping by tetravalent metals such as tin or titanium has also captured attention because of the occurrence of titanomagnetite in nature [1, 3–5], and because the substitution of tetravalent ions can be used to stabilize γ-Fe_2O_3 against transformation into α-Fe_2O_3 at elevated temperatures [2].

Any important question associated with the structural and physical properties of these materials concerns the occupation by the dopant of either the tetrahedral or the octahedral sites and its influence on magnetization [11]. We have previously examined these properties in tin- and titanium-doped γ-Fe_2O_3 [11] and in the present work we report on the preparation of ruthenium-doped γ-Fe_2O_3 and the influence of the local coordination of the dopant ions on the magnetic properties, including the effect of the dopant on the canting angle. We also report on the influence of ruthenium on the γ-Fe_2O_3 to α-Fe_2O_3 phase transition and the Morin temperature of the transformed sample.

2. Experimental details

Ruthenium-doped γ-Fe_2O_3 was prepared by adding aqueous ammonia to a 2:1 mixture of aqueous solutions of iron(III) chloride hexahydrate and iron(II) chloride tetrahydrate which had been mixed with an aqueous solution of ruthenium(III) chloride. The mixture was boiled under reflux (3 h), the precipitate removed by filtration, washed with 95% ethanol until no chloride ions could be detected in the washings by silver nitrate solution, and heated in air at 250 °C (12 h).

X-ray powder diffraction data were recorded with a Siemens D5000 diffractometer in reflection mode using Cu Kα radiation. The ^{57}Fe Mössbauer spectra were recorded at 4.2, 77 and 285 K with a conventional constant acceleration spectrometer in transmission geometry using a 400 MBq ^{57}Co/Rh source. A similar arrangement was used for the *in situ* study of the γ-Fe_2O_3 to α-Fe_2O_3 phase transformation and for the determination of the Morin transition in ruthenium-doped α-Fe_2O_3. Some ^{57}Fe Mössbauer spectra were also recorded in the presence of an applied field using a cryomagnetic device where the applied field is oriented parallel to the γ-ray beam. All the isomer shift data are reported relative to that of α-iron at room temperature. The ruthenium K-edge x-ray absorption spectra were recorded on station 9.2 at the SRS at the Daresbury Laboratory. The ring current varied between 220 and 120 mA in the 2 GeV storage ring. The beamline used a Si(220) double crystal monochromator which was detuned by 40% to remove higher order harmonics. The monochromator was calibrated with a ruthenium dioxide powder sample, the edge of which was taken to be at 22 128.2 eV. The ground powder sample was sprinkled onto adhesive tape and data were collected in transmission mode. The data were reduced using the SRS programs EXCALIB and EXBROOK. EXAFS data analyses were performed using the program EXCURV98 [12]. Phase shifts were calculated *ab initio* using Hedin–Lundqvist exchange potentials and von Barth ground state potentials. The refinement was performed using single scattering with coordination numbers fixed from the iron sites in γ-Fe_2O_3. The shell radii were allowed to vary in the fitting process. The fit index R quoted in table 1 is defined by $R = \sum_i [(1/(\sigma_i))(|\text{experiment}(i) - \text{theory}(i)|] \times 100\%$ where $1/(\sigma_i) = [k(i)]^3/(\sum_i [k(i)]^3 |\text{experiment}(i)|)$ [12], where $k(i)$ is the wavevector amplitude for the ith point.

Table 1. Table of neighbouring atoms around Fe sites from XRD based on best-fit parameters for ruthenium K-edge EXAFS recorded from ruthenium-doped γ-Fe_2O_3 at 298 K. The table includes first coordination sphere oxygen atoms and iron atoms within a 4 Å radius, all atoms with interatomic separations which differ by less than 0.1 Å are treated as one coordination shell.

Fe1 (Å)		Fe2 (Å)		Fe3 (Å)		Fe4 (Å)	
4O	1.88	6O	2.02	3O	1.93	4O	2.03
2.33Fe	3.35	4.66Fe	3.09	3O	2.11	2O	2.33
4Fe	3.44	6Fe	3.45	0.33Fe	2.72	2Fe	2.72
6.33Fe	3.53			4.33Fe	3.02	4Fe	2.98
				3Fe	3.38	2Fe	3.34
				3Fe	3.52	2Fe	3.49
						2Fe	3.66

3. Results and discussion

3.1. XRD, XANES and EXAFS

The broad peaked x-ray powder diffraction pattern recorded from ruthenium-doped γ-Fe_2O_3, which was shown by inductively coupled plasma (ICP) analysis to contain 3.12% ruthenium, was characteristic of a γ-Fe_2O_3-related structure and showed no evidence of other crystalline phases. This, together with the mean particle size of about 15 nm as determined by the Scherer method, was unequivocally confirmed by ^{57}Fe Mössbauer spectroscopy (see later).

The position of the x-ray absorption edge recorded from ruthenium-doped γ-Fe_2O_3 of 22 128.3 $\pm$ 0.2 eV was measured following measurement of ruthenium dioxide and demonstrates that ruthenium is present as Ru^{4+}.

The fitting of the EXAFS was based on the structure of γ-Fe_2O_3 [13], which contains one tetrahedral iron site, designated here as Fe1, and three octahedral iron sites. Two of the octahedral iron sites (designated as Fe2 and Fe3) are fully occupied whilst the third (designated as Fe4) is $\frac{1}{3}$ occupied. The results of the EXAFS analyses are shown in table 1 together with the distances from ruthenium to neighbouring oxygen and iron ions calculated from diffraction data for four sites, Fe1 to Fe4. Figure 1 shows the Ru K-edge EXAFS.

Each of the four sites was used as a starting model in the analysis with appropriate groupings of Debye–Waller factors. Oxygen atoms not in the first coordination sphere were ignored. Only when site Fe2 was used as the starting point, was a minimum achieved in which the shells retained reasonable values relative to their idealized values obtained from diffraction data. The iron ions in the second coordination sphere were at a slightly further distance (3.09 Å) than indicated by the diffraction results (3.00 Å), and the Debye–Waller factor for this shell was slightly larger than one might expect. This may be due to some local distortion in the structure about the sites in which ruthenium is located, or could be indicative that not all the ruthenium is in the same site. Thus while the EXAFS strongly suggest that ruthenium is located in site Fe2, partial occupation of another site cannot be ruled out, although this is likely to be a minor, $<$20%, contribution. The result is similar to that observed in tin-doped γ-Fe_2O_3, but contrasts with that recorded [11] from titanium-doped γ-Fe_2O_3 where the dopant was found to mainly occupy the F4 sites.

3.2. Mössbauer spectroscopy

The ^{57}Fe Mössbauer spectra recorded at 285 K from the ruthenium-doped γ-Fe_2O_3 following heating at 700 and 800 K are shown in figure 2. Spectrum (a), which was recorded from the

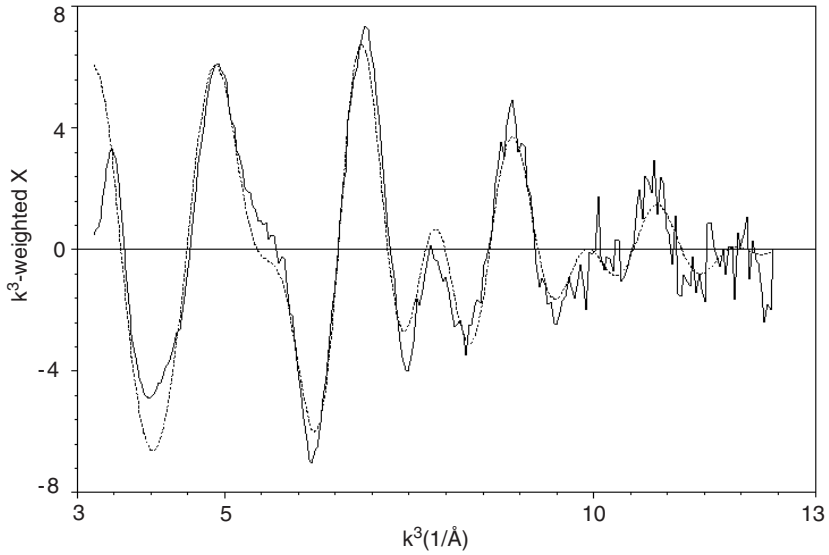

Figure 1. Ruthenium K-edge EXAFS recorded from ruthenium-doped γ-Fe_2O_3 (—— experimental, - - - - theoretical).

sample before any treatment, consisted of a magnetic component, which could be fitted with a distribution of sextets with magnetic hyperfine parameters characteristic of γ-Fe_2O_3 and a paramagnetic component indicative of some of the sample being in a superparamagnetic state at room temperature. Spectrum (b) was recorded at 285 K after treatment at 700 K for 42 h. Two significant changes were observed. The paramagnetic component had largely disappeared most likely as a result of sintering effects, and a new sextet, with a line width of 0.29 mm s^{-1} and a magnetic hyperfine field of 52.7 T was needed to achieve a satisfactory fit to the spectrum. This sextet had a quadrupole shift, $\Delta = +0.39$ mm s^{-1}, an isomer shift, $\delta = +0.37$ mm s^{-1} and accounted for about 38% of the spectral area. These hyperfine parameters are consistent with ruthenium-doped α-Fe_2O_3 below the Morin transition. A subsequent scan showed that the Morin transition, T_M, takes place between 390 and 410 K. It has been observed that whereas most cations cause a lowering of the Morin transition temperature, T_M, in hematite, Ru^{3+}, Rh^{3+} and Ir^{4+} are known to increase the Morin temperature [14–16]. Further heating to 800 K gave a spectrum (c), which could not be fitted to parameters characteristic of γ-Fe_2O_3 but was fitted to parameters typical of α-Fe_2O_3 and was thereby indicative of the phase transition from γ-Fe_2O_3 to α-Fe_2O_3 at higher temperature than normally expected [1, 5]. The result endorses our previous observations [2, 17] that dopant ions can increase the temperature at which γ-Fe_2O_3 is converted to α-Fe_2O_3.

The doublet seen in the spectrum (a) recorded at 285 K showed that some of the iron, at least, is present in a superparamagnetic state at room temperature. This conclusion was confirmed by the spectra recorded at 77 and 4.2 K (figure 3). The spectrum recorded at 77 K showed no paramagnetic contribution and at least three sextets, or a discrete distribution of the magnetic hyperfine fields, were needed to fit the spectrum satisfactorily, indicating a distribution in particle size, presumably of around 15 nm, determined by x-ray diffraction. At 4.2 K the spectrum was best fitted with two sextets with the same quadrupole shift but slightly different isomer shifts. The same quadrupole shift is consistent with the presence of both tetrahedral and octahedral iron sites but the lack of resolution prevented an accurate estimation

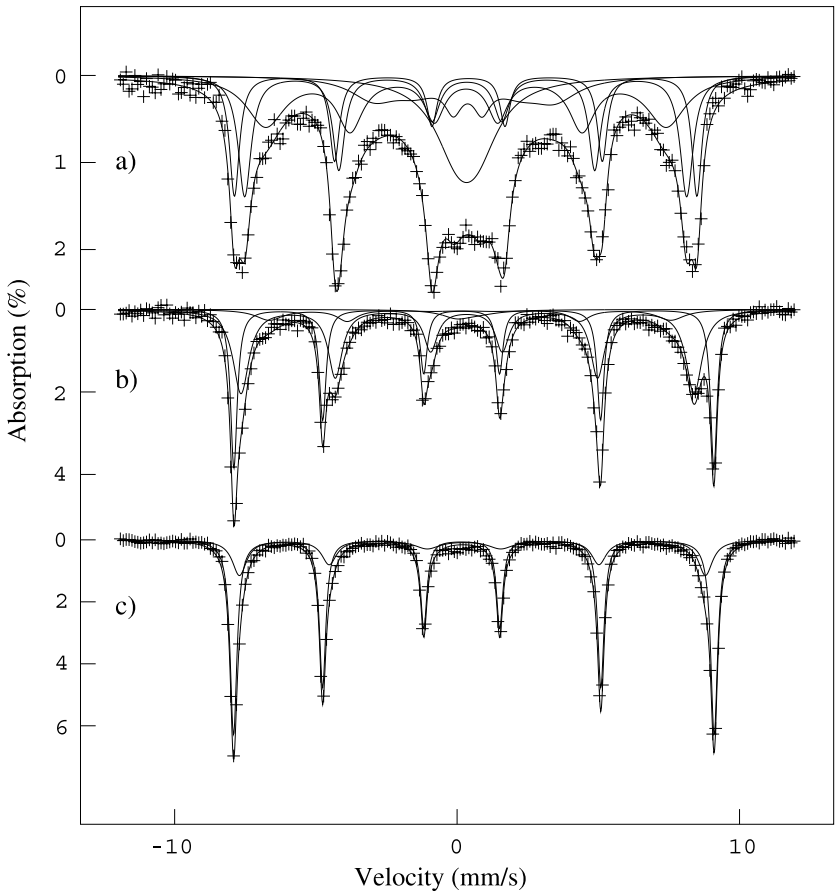

Figure 2. ^{57}Fe Mössbauer spectra recorded from ruthenium-doped γ-Fe_2O_3 (a) at 285 K, (b) after 42 h at 700 K, (c) after 28 h at 800 K.

Table 2. ^{57}Fe Mössbauer parameters recorded at 285, 77 and 4.2 K.

T (K)	Spectral component	δ (mm s^{-1}) ($\pm$0.02)	Γ (mm s^{-1}) ($\pm$0.02)	Δ or 2ε (mm s^{-1}) ($\pm$0.02)	B_{hf} (T) ($\pm$0.2)	Area ratio % ($\pm$2)
285	'1st sextet'	0.36	0.4	0	50	20
	'2nd sextet'	0.34	0.6	0	48.5	25
	Broad distribution of 'sextets'	0.3–0.4		0	40–45	30
	doublet	0.34	1.2	0.7		25
77	'1st sextet'	0.46	0.54	−0.02	52.2	50
	'2nd sextet'	0.43	0.56	0.01	49.3	32
	'3rd sextet'	0.49	0.88	0.12	44.6	18
4.2	Octahedral	0.47	0.46	−0.02	53.1	56
	Tetrahedral	0.42	0.54	−0.02	50.9	44

of the proportions. No divalent iron-containing species were observed. The main hyperfine parameters for the discrete sextets and doublets are given in table 2.

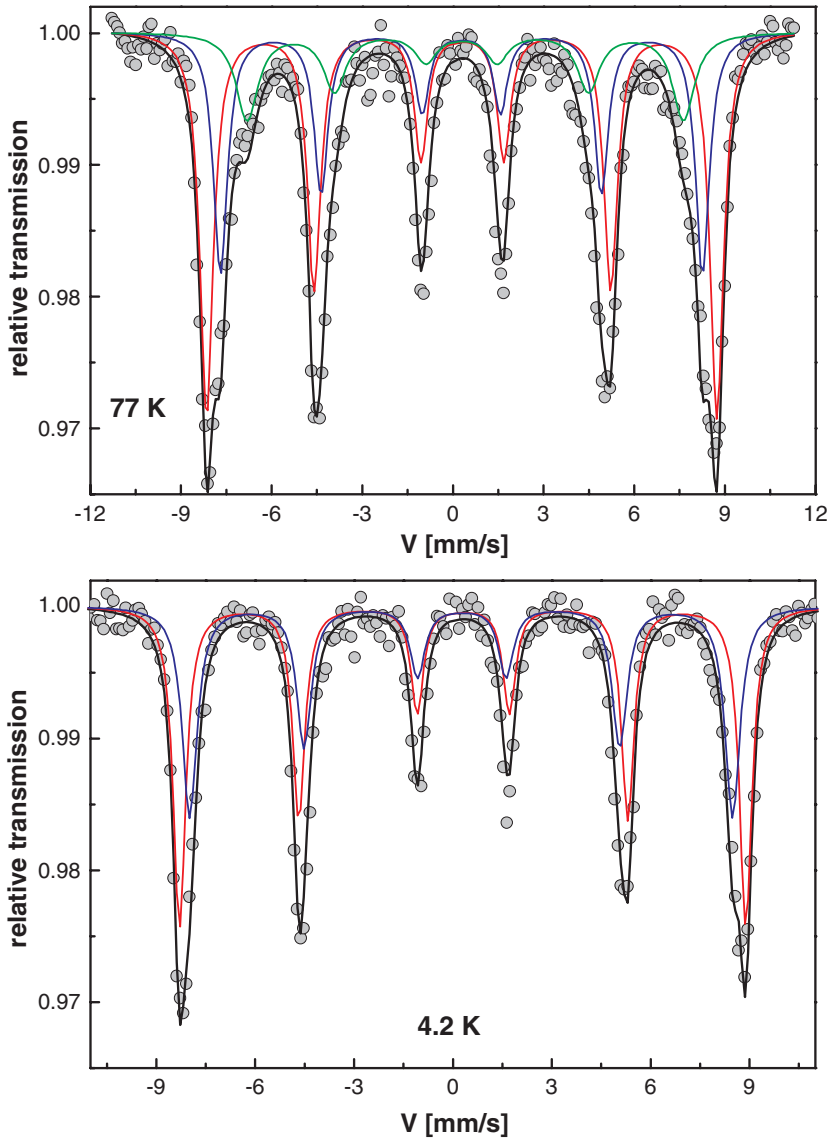

Figure 3. ^{57}Fe Mössbauer spectra recorded at 77 and 4.2 K.

To examine the effect of the dopant, the ^{57}Fe Mössbauer spectrum was recorded at 10 K in an external magnetic field of 6 T parallel to the direction of the γ-ray beam (figure 4). A splitting of the outermost lines 1 and 6 was clearly evident and a significant decrease in the intensities of lines 2 and 5 was observed. The spectrum was best fitted with two discrete distributions of the magnetic hyperfine field corresponding to the octahedral and tetrahedral iron sites. Within each distribution the isomer shift and the quadrupole shift were considered to be identical for all sextets. The isomer shift for the two distributions differs by approximately 0.1 mm s^{-1}, which is consistent with the difference usually observed in this type of oxide. The minima in the positions of lines 2 and 5 indicate a non-vanishing component of the hyperfine field perpendicular to the applied field. The ratio of the areas of the lines (2, 5) to the lines (1, 6)

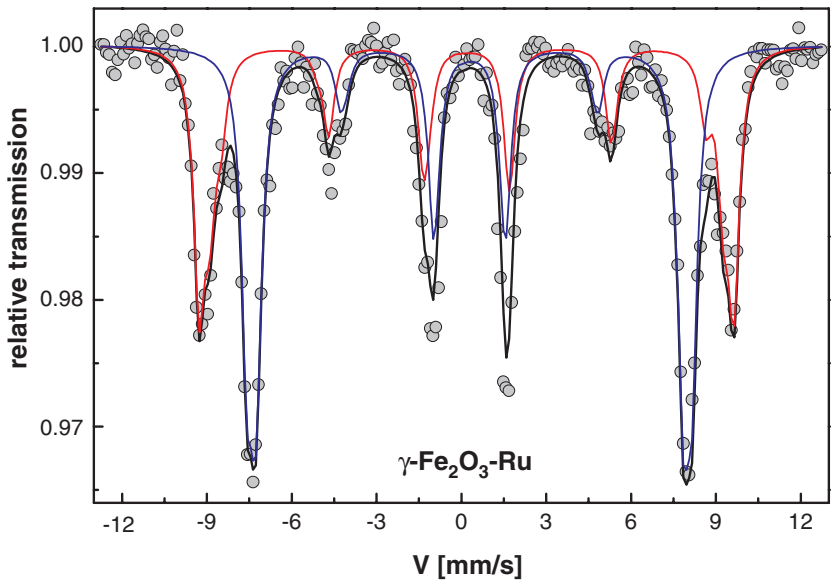

Figure 4. ^{57}Fe Mössbauer spectrum recorded at 10 K in an external magnetic field of 6 T parallel to the γ-radiation.

is related to the canting angle between the hyperfine field and the external field [7, 18, 19]. Indeed, the effective field $\boldsymbol{B}_{eff}$ at the iron nucleus results from the vector sum of the hyperfine field $\boldsymbol{B}_{hf}$ and the applied field $\boldsymbol{B}_{app}$. If $\boldsymbol{B}_{eff}$ is inclined at an angle ϑ from the γ-ray direction, the peak areas are in the ratio $3{:}2p{:}1{:}1{:}2p{:}3$ with $p = 2\sin^2\vartheta/(1+\cos^2\vartheta)$. By normalizing the total area $\Sigma A_{i,7-i} = 1$, the area of each of the lines 2, 5 is $A_{2,5} = 1/4\sin^2\vartheta$. The values of the mean hyperfine magnetic field at the octahedral and tetrahedral sites can then be estimated from those of the in-field effective field using the relationship

$$\langle B_{hf}^2\rangle = \langle B_{eff}^2\rangle + B_{app}^2 - 2\times\langle B_{eff}\rangle\times B_{app}\times\cos\langle\vartheta\rangle \tag{1}$$

where the angle $\langle\vartheta\rangle$ defines the direction of the mean effective field with respect to the γ-ray direction.

Within each distribution the angle ϑ, which defines the direction of the effective field with respect to the γ-ray direction, i.e. the applied field direction, was assumed free during the fitting procedure. The distributions enable an average value of both $\langle B_{eff}\rangle$ and $\langle\vartheta\rangle$ to be estimated independently for the tetrahedral and octahedral components. The results are shown in table 3. The results show a good agreement between the values of the angles and their corresponding effective field in comparison to the hyperfine field. For example, for the tetrahedral iron site, the effective field corresponding to iron moments oriented antiparallel to the applied field is associated with the small value of ϑ, (i.e. $B_{eff} = B_{hf} + B_{app}$), while the lowest effective fields are associated with an angle ϑ close to 90° which is consistent with large canting. However, the main difficulty with fitting concerns the estimation of the limits of the distribution, especially the lower limit of the tetrahedral component and the higher limit of the octahedral component. The fitting model was refined by using different values of applied field and the difference between the two values of isomer shift considered as a satisfactory test. The results from the fitting of the spectrum and the calculation of the mean angle ϑ (table 3) showed that the canting angles for the Fe^{3+} ions in γ-Fe_2O_3 can be determined as 24° for those in octahedral sites and 33° for those in tetrahedral sites. This is similar to values recorded from

Table 3. ^{57}Fe Mössbauer parameters at 10 K in an external magnetic field of 6 T parallel to the γ-rays.

Sextet	δ mm s^{-1} ($\pm$0.02)	Δ or 2ε mm s^{-1} ($\pm$0.02)	B_{eff} (T) ($\pm$0.2)	Area ratio % ($\pm$2)	Canting angle (ϑ) ($\pm$5)	B_{hf} (T) ($\pm$0.2)
Octahedral	0.52	0.00	47.5	56	24	53.0
Tetrahedral	0.42	−0.02	56.4	44	33	51.5

tin-doped γ-Fe_2O_3 (30° and 35° respectively), but different from those observed for titanium-doped γ-Fe_2O_3 and undoped γ-Fe_2O_3, which showed the canting angle to be significantly greater for the octahedral sublattice than the tetrahedral sublattice [11].

The effect of the doping on the area ratio can be estimated from the applied field measurement. In a previous study [11] of pure γ-Fe_2O_3, 60% of the area was assigned to the sextet corresponding to iron in octahedral sites and 40% to the sextet corresponding to iron in tetrahedral sites. This is in reasonable agreement with the 5/3 area ratio expected from the structure of pure γ-Fe_2O_3. The preferential substitution of iron on the octahedral site decreases this ratio with increasing amounts of ruthenium doping. This was confirmed by the decrease in area ratio from 60/40 for pure γ-Fe_2O_3 to 56/44 for the ruthenium-doped γ-Fe_2O_3.

4. Conclusions

The EXAFS measurements show that the ruthenium ions go into the octahedral sites of γ-Fe_2O_3 as Ru^{4+} and is most likely located in the fully occupied (Fe2) site.

The mean canting angles for the Fe^{3+} ions in the ruthenium-doped γ-Fe_2O_3 were determined to be 24° for those in octahedral sites and 33° for those in tetrahedral sites. This is similar to values recorded from tin-doped γ-Fe_2O_3 (30° and 35° respectively), but different from those observed for titanium-doped γ-Fe_2O_3 and undoped γ-Fe_2O_3, which showed the canting angle to be significantly greater for the octahedral sublattice than the tetrahedral sublattice [11].

At 700 K a transformation of ruthenium-doped γ-Fe_2O_3 to ruthenium-doped α-Fe_2O_3 was observed. The Morin transition temperature, T_M, of the ruthenium-doped α-Fe_2O_3 was determined to be 400 K, which is about 140 K higher than the T_M usually reported for pure α-Fe_2O_3 (hematite).

Acknowledgments

We wish to acknowledge the use of the EPSRC Chemical Database Service at Daresbury Laboratory. We also wish to thank Dr I Ayub for initially preparing the sample

References

[1] Vandenberghe R E and De Grave E 1989 Mössbauer effect studies of oxidic spinels *Mössbauer Spectroscopy Applied to Inorganic Chemistry* vol 3, ed G J Long and F Grandjean (New York: Plenum) pp 59–182
[2] Berry F J, Greaves C, Helgason Ö and McManus J 1999 *J. Mater. Chem.* **9** 223–6
[3] Moukarika A, O'Brian F and Coey J M D 1991 *Geophys. Res. Lett.* **18** 2043–6
[4] Resende M, Allan J and Coey J M D 1986 *Earth Planet. Sci. Lett.* **78** 322
[5] Steinthorsson S, Helgason Ö, Madsen M B, Bender Koch C, Bentzon M D and Mørup S 1992 *Mineral. Mag.* **56** 185–99
[6] Pollard R J 1988 *Hyperfine Interact.* **41** 509–12

[7] Da Costa G M, De Grave E, Bowen L H, Vandenberghe R E and De Bakker P M A 1994 *Clay Clay Miner.* **42** 628–33
[8] Da Costa G M, De Grave E and Vandenberghe R E 1998 *Hyperfine Interact.* **117** 207–43
[9] Anamtharaman M R, Malini K A, Sindhu P D, Sindhu S and Keer H V 1999 *Indian J. Pure Appl. Phys.* **37** 842–7
[10] Anamtharaman M R, Scsham K, Shringi S N and Keer H V 1981 *Bull. Mater. Sci.* **6** 59
[11] Helgason O, Greneche J M, Berry F J, Morup S and Mosselmans F J 2001 *J. Phys.: Condens. Matter* **13** 10785–97
[12] Binsted N, Campbell J W, Gurman S J, Ross I and Stephenson P C 1998 Excurv98. CCLRC Daresbury Laboratory Computer Program
[13] Fletcher D A, McMeeking R F and Parkin D 1996 *J. Chem. Inf. Comput. Sci.* **36** 746–9
[14] Morrish A H 1994 *Canted Antiferromagnetism: Hematite* (Singapore: World Scientific) p 125ff
[15] Liu J Z and Fan C L 1984 *Phys. Lett.* A **105** 80
[16] Kileinikov G I, Maksimov Y V, Dudoladov V V, Suzdalev I P, Brodskaya I G and Dmitrenko L M 1989 *Kinetics Catal.* **30** 815
[17] Helgason O, Berry F J, Jonsson K and Skinner S J 1996 *Proc. Int. Conf. on the Applications of the Mössbauer Effect* ed I Ortalli and S I F Bologna (Bologna: Societa Italiana di Fisica) p 59
[18] Tronc E, Prené P, Jolivet J P, Dormann J L and Greneche J M 1998 *Hyperfine Interact.* **112** 97–100
[19] Morales M P, Serna C J, Bødker F and Mørup S 1997 *J. Phys.: Condens. Matter* **9** 5461–7